

Modeling Global Environmental Fate and Quantifying Global Source–Receptor Relationships of Short-, Medium-, and Long-Chain Chlorinated Paraffins

Chengkang Chen, Li Li, Shaoxuan Zhang, Jianguo Liu,* and Frank Wania*



Cite This: *Environ. Sci. Technol. Lett.* 2024, 11, 626–633



Read Online

ACCESS |

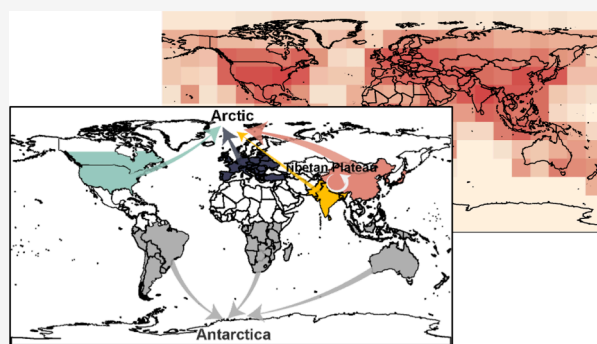
Metrics & More

Article Recommendations

Supporting Information

ABSTRACT: Decades-long emissions and long-range transport of chlorinated paraffins (CPs) have resulted in their pervasive presence in the global environment. The lack of an understanding of the global distribution of short-, medium-, and long-chain CPs (SCCPs, MCCPs, and LCCPs) hinders us from quantitatively tracing their origins in remote regions. Using the BETR-Global model and historical emission estimates, we simulate the global dispersion of CPs from 1930 to 2020. Whereas contamination trends in the main contaminated regions (East Asia, Europe, North America, and South Asia) diverge, CP concentrations in the Arctic, Antarctica, and the Tibetan Plateau all increase. By 2020, East Asian, European, and North American emissions contributed 38%, 26%, and 18% of CP contamination in the High Arctic, respectively, while Southern hemispheric emissions and emissions around the Tibetan Plateau primarily contribute to CP contamination in central Antarctica and on the Plateau, respectively. Our results emphasize the important contribution of (i) European and North American emissions to historical CP contamination in remote regions and current MCCP and LCCP contamination in the High Arctic and (ii) East Asian emission to current SCCP and MCCP contamination of all three remote regions. These results can help to evaluate the effectiveness of potential global and regional CP emission-reduction strategies.

KEYWORDS: SCCPs, MCCPs, LCCPs, environmental fate, source–receptor relationship, multimedia model



INTRODUCTION

Since the 1930s, the extensive production and use of chlorinated paraffins (CPs), including short-chain (SCCPs), medium-chain (MCCPs), and long-chain (LCCPs) CPs, have resulted in significant emissions into the environment.¹ By 2020, the cumulative global emissions of these synthetic chemicals were estimated to have reached approximately 5.2 million metric tons, which even surpasses the global cumulative production of polychlorinated biphenyls that notoriously have caused numerous environmental and health problems around the world.^{1–3} Such substantial emissions have not only caused pervasive environmental contamination in regions where CPs are produced and used but the atmosphere and marine currents have also conveyed quantities worthy of concern to distant regions.^{4–6} Due to this potential for long-range transport,^{7–9} coupled with environmental persistence,^{10–12} bioaccumulation,^{13,14} and adverse effects^{15–17} on ecosystems and humans, CPs have been recognized as global pollutants of concern. Consequently, national agencies and international treaties have actively evaluated and regulated CPs.^{18–20} SCCPs are regulated as persistent organic pollutants (POPs) since 2017,¹⁹ and the POP Review Committee has recently determined that MCCPs meet all four criteria for regulation

under the Stockholm Convention.²⁰ Given this context, it is imperative to comprehensively understand the environmental fate and contamination of CPs on a global scale.

In recent decades, monitoring studies have enhanced our understanding of the environmental fate of CPs.^{4–6,8,21–23} For example, elevated environmental concentrations of SCCPs, MCCPs, and LCCPs have been reported in China,^{24,25} and their presence in remote Arctic, Antarctic, and Tibetan Plateau regions has been confirmed.^{5,9,26,27} However, environmental measurements are often scattered in time and space and may not represent comprehensively the average occurrence within a region, a crucial factor for environmental risk assessment.²⁸ Deriving spatial distributions from environmental measurements reported by different studies is challenging because of divergent time periods of sampling in different regions and

Received: April 18, 2024

Revised: May 20, 2024

Accepted: May 21, 2024

Published: May 23, 2024



inconsistency in analytical methods and reporting conventions. The available measurements do not reach far back in time to deduce the long-term environmental fate of CPs, which is crucial for assessing the effectiveness of possible emission-reduction actions in the future. Therefore, there remains a need for a holistic view of the spatial and temporal trends in the environmental fate of CPs on a global scale.

In particular, while existing studies have independently established the occurrence of CPs in both source regions and remote receptor regions,^{5,6,9} a quantitative understanding of the relationship between individual source regions and receptor regions is missing. Such source–receptor relationships are particularly complex for CPs given that (i) temporal trends of emissions in different source regions diverge, for example, while CP emissions in Western Europe peaked and dominated globally in the 1980s, emissions in China did not surge until the 2000s,¹ and (ii) the relative abundance of SCCPs, MCCPs, and LCCPs in emissions varies across regions and time, for example, while SCCP emissions have peaked and begun decreasing before the 1990s in North America, the MCCP and LCCP emissions continue to increase and now dominate CP emissions.¹ Developing source–receptor relationships should aid in identifying the primary sources of CP contamination in remote regions and enhance the understanding of how that contamination responds to the evolving use and emissions of CPs. Such a capability would support the goals of multilateral environmental agreements aiming to reduce or eliminate emissions that impact remote ecosystems.^{19,29}

Multimedia fate and transport models linking the environmental fate of CPs with emission inventories can complement measurements in the task of establishing source–receptor relationships.^{30,31} Taking advantage of the availability of global time-variant emission inventories for the CPs,¹ we simulate here their long-term global environmental fate and explore how their environmental occurrence changes across environmental compartments, regions, and over time. Furthermore, we quantify the relative contribution of emissions from different source regions to the contamination in three remote regions and uncover how these contributions evolve over time.

METHODS AND MATERIALS

Fate Modeling Strategy. We applied the global, multimedia model BETR-Global (Version 2.16)^{32,33} to simulate the environmental fate of SCCPs, MCCPs, and LCCPs. BETR-Global, which has previously been evaluated and successfully applied to SCCPs³⁴ and other POP-like chemicals,^{35–40} divides the global environment into 288 15° latitude × 15° longitude grid cells, with each cell containing seven interconnected compartments (upper air, lower air, vegetation, freshwater, coastal water, soil, and sediment). Figure S1 in the Supporting Information shows the model structure and environmental processes considered in BETR-Global. When supplied with emission estimates, equilibrium partition ratios between air, water, and octanol (K_{AW} , K_{OA} , and K_{OW}), environmental degradation half-lives, internal energies of phase change, and activation energies, the model calculates annually averaged masses and concentrations in all 2016 environmental compartments. Here we ran the model with input parameters resolved at the level of 21 carbon-specific CP homologue groups. Results for SCCPs, MCCPs, and LCCPs were obtained as the sum of model results for the corresponding homologue groups.

In a baseline scenario, BETR-Global was first run with the complete CP emission estimate. To establish global source–receptor relationships we delineated four source regions (Figure S1): North America (corresponding to cells 52–56, 76–80), Europe (60–63, 84–87), East Asia (91–94, 115–118), and South Asia (113–114, 137–138) and three remote regions: the High Arctic (1–24), central Antarctica (265–288), and Tibetan Plateau (90). Running the model four more times with emissions solely occurring in one of the source regions allowed the attribution of the CPs in each of the remote regions to specific source regions.³⁰ In this analysis, any secondary emissions of CPs previously deposited in a surface compartment are attributed to the source regions of their original emission.

Emission Estimates and Physicochemical Properties.

We employ the global, time-varying, region-specific emission inventories for the CPs for the period 1930–2020 by Chen et al.¹ Emissions, resolved at the level of 21 carbon-specific CP homologue groups,^{34,41} were assumed to occur into the lower air, freshwater, and soil compartments.¹ Regional emissions arising from production, industrial processing, in-use, and waste treatment were geographically allocated into specific grid cells based on surrogate data on the production capacities and locations of CP manufacturers, gross domestic product, population density, and waste generation density, respectively.¹

To obtain physicochemical properties, we used a Monte Carlo method^{42,43} to generate a set of Simplified Molecular-Input Line-Entry System (SMILES) strings representing CPs (See detailed descriptions in Table S1 and elsewhere^{42,44,45}). These SMILES strings were then used to predict the K_{OW} , K_{OA} , and K_{AW} and heats of phase transfer between these phases by a COSMO-RS-trained fragment contribution model.⁴² Degradation half-lives were predicted using AOPWIN and BIOWIN within EPI Suite.^{46,47} Comprehensive details on property data, calculations, and assumptions are provided in Table S1. Default values in BETR-Global were used for other required input data.³²

RESULTS AND DISCUSSION

Model Performance Evaluation. By comparing the model results with measurements reported in the literature (details in Figure S2), we observe that over 79% of the modeled concentrations fall within an order of magnitude of measured values. The model also succeeds in reproducing temporal trends measured in soil and sediment cores (Figure S2),^{10,12,48–50} e.g., a decreasing trend of SCCPs in Swedish coastal sediments and Swiss soils in recent years (Figure S2c,d), and general increasing and steady trends of MCCPs in Swedish coastal sediments and Swiss soils, respectively, after the 1990s (Figure S2f,g).^{12,48} Considering the large uncertainty or variation in the measurements due to different analytical methods being applied among the studies, this agreement indicates satisfactory model performance in reproducing environmental concentrations of CPs and their temporal trends.

Environmental Occurrence in Source Regions. Our modeling results unveil the spatial global environmental distribution of SCCPs, MCCPs, and LCCPs (Figure S3). Consistent with relatively high use volume and emissions in East Asia, Europe, North America, and South Asia,¹ these four regions were the “hotspots” of CP contamination, containing 17%, 16%, 31%, and 12% of the total mass present in the global environment by 2020, respectively (Figure S4).

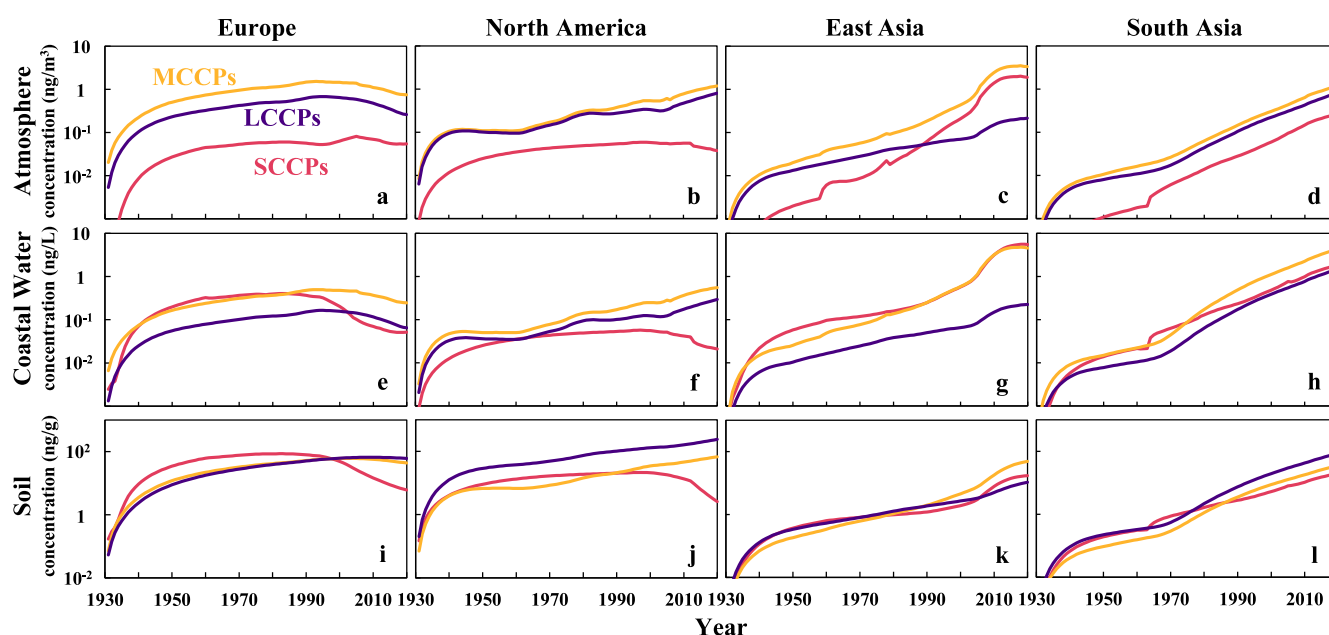


Figure 1. Temporal evolution of SCCP, MCCP, and LCCP concentrations in atmosphere (lower air), coastal water, and soil within BETR-Global cells 61 (panels a, e, and i), 79 (panels b, f, and j), 92 (panels c, g, and k), and 114 (panels d, h, and l), which represent Europe, North America, East Asia, and South Asia, respectively.

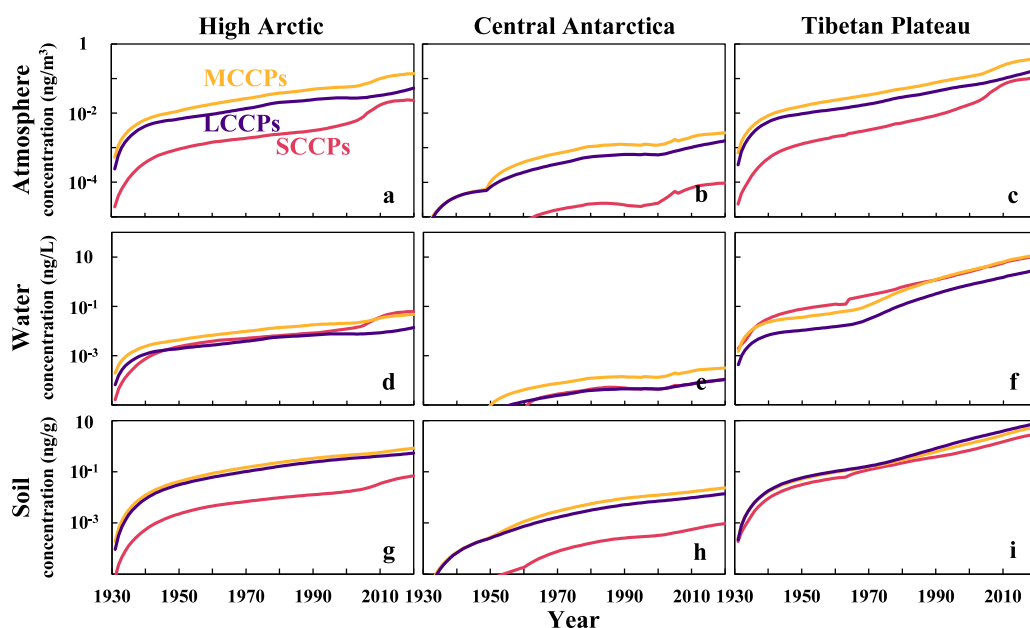


Figure 2. Temporal evolution of SCCP, MCCP, and LCCP concentrations in the lower atmosphere, coastal water, and soil within the High Arctic, central Antarctica, and Tibetan Plateau from 1930 to 2020. Panel f shows concentrations in fresh water since there is no coastal water on the plateau.

Temporal trends of CP concentrations in air, coastal water, and soil deviate considerably between these four regions (Figure 1). While concentrations in East and South Asia increase substantially, those in Europe have peaked and begun to decrease since the 2000s. In North America, concentrations of SCCPs started decreasing after the 1990s, but those of MCCPs and LCCPs continue to increase remarkably. These trends, including the relative abundances of SCCPs, MCCPs, and LCCPs, closely match emission trends in these source regions (Figure S5). For example, in Europe, the predominant use of SCCPs in metalworking fluids results in more emissions

into water and soil, leading to higher concentrations of SCCPs in coastal water and soil, whereas MCCPs, primarily applied in PVC products, dominate emissions into air and consequently air concentrations.¹

As for multimedia distributions, Figure 1 illustrates that within the same region, despite MCCP emissions exceeding SCCP emissions to water in East Asia (Figure S5), the relative enrichment of MCCPs compared to SCCPs is lower in coastal water since more MCCPs partition into soil or sediment due to their higher K_{OW} . In addition, within the same region, the relative enrichment of LCCPs is higher in soil than in air due

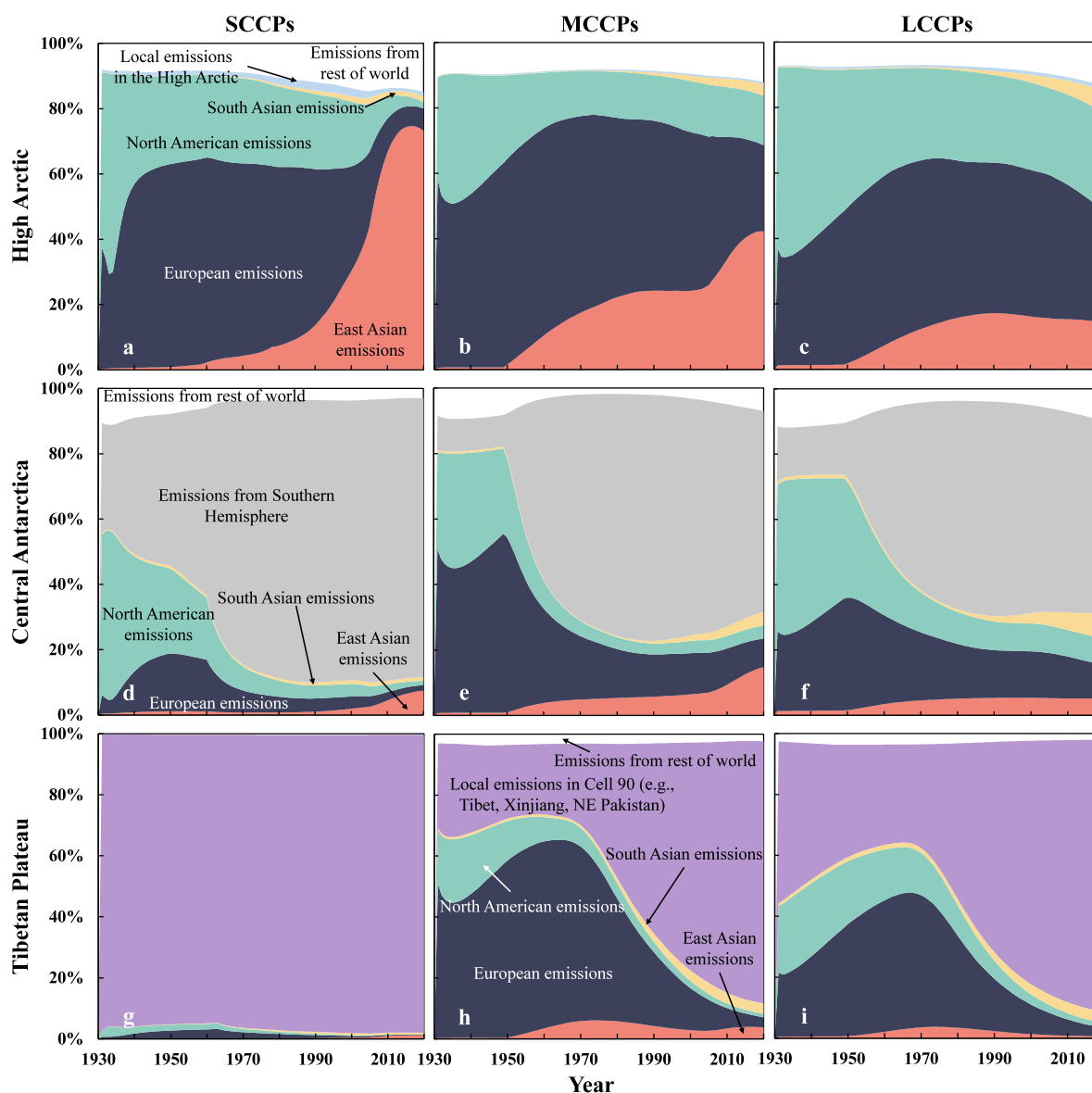


Figure 3. Temporal trends of the relative emission contributions of East Asia, Europe, North America, and South Asia to SCCP, MCCP, and LCCP contamination in the High Arctic, central Antarctica, and Tibetan Plateau. The blue, gray, and purple areas designate the contributions of emissions in the local High Arctic, Southern Hemisphere, and cell no. 90, respectively, while the white areas designate the contribution of emissions from the rest of world.

to their higher K_{OA} , causing them to preferentially settle onto soils. These trends are further reflected in the compartment-specific homologue profiles (Figure S6), where lighter CP homologues (e.g., C_{10-15} -CPs) are more prevalent than heavier homologues (e.g., C_{18-30} -CPs) in air, and the opposite holds in soil.

Environmental Occurrence in Remote Regions.

Contrasting with the remarkably divergent temporal trends in source areas, concentrations of CP are increasing in all three remote regions from 1930 to 2020 (Figure 2). This aligns with reported measurements, such as an ascending trend in atmospheric concentrations of SCCP and MCCP during the period 2013–2020 in Arctic Norway⁵¹ and a slight increase in atmospheric SCCP and MCCP concentrations during the period 2014–2018 on the Fildes Peninsula, Antarctica.⁵ The temporal trends in remote regions reflect the combined influence of emissions in different source regions. For instance, while atmospheric SCCP concentrations in the High Arctic

follow a trend similar to that of SCCP emissions in East Asia after the 2000s, the corresponding MCCP concentrations align with atmospheric MCCP emissions in Europe before the 2000s and, subsequently, with those in North America. Consequently, a quantitative analysis of source–receptor relationships is necessary for a more comprehensive understanding of the temporal evolution of concentrations in remote regions (see the section below).

Comparing CP homologue profiles in the remote regions (Figure S7) with those in the source regions (Figure S6) reveals that shorter-chain CPs, notably C_{10-14} -CPs, are more abundant in remote environments than in source regions. This reflects the higher potential of these lighter CPs to reach remote regions. Among CPs reaching remote regions, the heavier, longer-chain CPs, notably C_{20-30} -CPs, are more prone to partition to surface media such as soil. This is further evident when comparing Figure 2a–c with Figure 2g–i, where heavier LCCPs are more prevalent in soil than in the

atmosphere. Overall, these results underscore the fractionation and redistribution of CPs in the global environment due to diverging environmental behaviors between homologue groups.

Global Source–Receptor Relationships for Remote Regions. Figure 3 depicts the relative emission contributions of the four source regions to SCCP, MCCP, and LCCP contamination in the three remote regions. Overall, emissions from the selected source regions contribute to over 80% of the contamination in the High Arctic, while these contributions are much lower in Antarctica and on the Tibetan Plateau (no more than 32% by 2020). This discrepancy arises from the facts that (i) all selected source regions are located in the Northern Hemisphere and interhemispheric atmospheric transport of CPs to Antarctica is limited; and (ii) contamination on the Tibetan Plateau is predominantly influenced by the local emissions within cell 90. Additional simulations indicate that emissions from the Southern Hemisphere and locally within cell 90 contribute over 59% and 86% to contamination in central Antarctica and on the Plateau by 2020, respectively (Figure 3). Importantly, this should not be interpreted as long-range transport of CPs to the Tibetan Plateau being negligible. A mass balance analysis (Table S2) shows that the mass of CPs transported to the Tibetan Plateau from other regions is of similar size to the mass transported into the High Arctic. However, emissions locally within cell 90 are much higher than local emissions within the High Arctic and Antarctica. One reason for this is that parts of industrial Xinjiang are falling within the confines of cell 90. Overall, these results underscore the importance of accurately assessing CP emission and fate in the Southern Hemisphere and around the Tibetan Plateau to mitigate the adverse effects of CPs in these remote regions.

Focusing on the relative importance of the selected source regions, our results highlight the historical contribution of European and North American emissions to CP contamination in remote regions (Figure 3), driven by their predominant emission fractions before the 2000s (Figure S8). For example, by 1990, emissions from these regions contributed ~71% of SCCP contamination in the High Arctic. Notably, the contribution of European emissions to CP contamination on the Tibetan Plateau are much larger than that of North American emissions due to westerly airflow in Northern midlatitudes, resulting in dominant eastward transport of CPs.⁵² Figure 3 also highlights the enduring dominance of European and North American contributions to MCCP and LCCP contamination in the High Arctic, with contributions reaching 41% and 64% of MCCP and LCCP contamination by 2020, respectively. Moreover, Figure 3 reveals the crucial role of East Asia in the SCCP and MCCP contamination of all three remote regions after the 2000s (e.g., contributing ~73% and 42% of SCCP and MCCP contamination, respectively, in High Arctic by 2020), attributed to the exponential increase in SCCP and MCCP emissions in China over the last two decades.^{1,53}

Research Limitations. Notwithstanding the insights gained from this study, we acknowledge important limitations in this work. While the quantum chemistry-based approach for predicting partition properties has an applicability domain that is not limited to specific groups of chemicals and has performed well in previous evaluations,^{42,43} the EPI Suite models might generate highly uncertain degradation properties outside their applicability domains. In addition, substantial data gaps may affect the emission estimates for the Southern

Hemisphere, where information about the production and use of CPs is rather inadequate.¹ This may lead to an underestimation of CP concentrations in the South. For example, modeled SCCP concentrations in Antarctica are lower than measurements on the Fildes Peninsula. However, this part of Antarctica has considerable human activity (research, tourism) possibly leading to concentrations higher than what can be expected for Antarctica overall.⁵

Owing to the low $15^\circ \times 15^\circ$ resolution of BETR-Global, cell 90 does not exactly overlap with the geographic Tibetan Plateau but also includes parts of Xinjiang and South Asia. Emissions within cell 90 do not necessarily refer to emissions occurring only on the Plateau itself but in its periphery (Figure S9). This may underestimate the South Asian contribution to contamination of the Plateau. Future research could opt for more highly spatially resolved models (e.g., Nested Exposure Model⁵⁴) to optimize source–receptor relationships. Different definitions of the Arctic and Antarctic regions may also alter the contributions of different source regions. For example, if one defines the Arctic as the region N of 60° (i.e., cells 1–48), the relative contributions of the four source regions decrease and that of local emissions will increase (Figure S10), since Northern Europe then becomes part of the Arctic. However, defining Antarctica as the region S of 60° (i.e., cells 241–288) has a limited impact on source contributions (Figure S10), since local emissions in cells 241–288 are estimated to be negligible (estimates of CP emissions from activities related to Antarctic research, tourism, and shipping are presently not available).

Moreover, the default assumptions of (i) equilibrium gas–particle partitioning and (ii) no degradation on atmospheric particles in BETR-Global can overestimate the atmospheric transport of CPs, especially for LCCPs, since they may not reach gas–particle partitioning equilibrium^{55,56} and/or undergo multiphase reactions⁵⁷ (albeit with possibly much slower rates^{58,59}). Our additional illustrative calculations with C_{25} –CPs either applying steady-state gas–particle partitioning⁵⁵ or allowing for degradation on particles (Figure S11) suggest that abandoning the default assumptions lowers atmospheric concentrations by less than an order of magnitude. Future global fate modeling efforts should seek to account for nonequilibrium partitioning (e.g., refs 55, 56) and multiphase chemistry in the atmosphere. Finally, BETR-Global does not appropriately represent snow and ice, which is a limitation, especially for the Arctic and Antarctic regions. As the presence of ice and snow may increase chemical concentrations in air but reduce long-range transport,⁶⁰ investigating how snow and ice influence global source–receptor relationships for CPs is a worthwhile future endeavor.

■ ASSOCIATED CONTENT

Supporting Information

The Supporting Information is available free of charge at <https://pubs.acs.org/doi/10.1021/acs.estlett.4c00306>.

Descriptions of BETR-Global model (Figure S1) and input parameters (Table S1); modeled vs measured concentration comparison (Figure S2); Spatial distribution of CP concentration and mass (Figure S3 and S4); Temporal evolution of emissions in source regions (Figure S5); homologue profile in source and receptor regions (Figure S6 and S7); steady-state mass balance of CPs in receptor regions (Table S2); CP emission

fractions of source regions to global emissions (Figure S8); geographical emission distribution in cell 90 (Figure S9); and assumption justifications (Figure S10 and S11) (PDF)

AUTHOR INFORMATION

Corresponding Authors

Jianguo Liu – State Key Joint Laboratory for Environmental Simulation and Pollution Control, College of Environmental Sciences and Engineering, Peking University, Beijing 100871, China; orcid.org/0000-0002-8878-588X; Email: jgliu@pku.edu.cn

Frank Wania – Department of Physical and Environmental Sciences, University of Toronto Scarborough, Toronto M1C 1A4 Ontario, Canada; orcid.org/0000-0003-3836-0901; Email: frank.wania@utoronto.ca

Authors

Chengkang Chen – Department of Physical and Environmental Sciences, University of Toronto Scarborough, Toronto M1C 1A4 Ontario, Canada; State Key Joint Laboratory for Environmental Simulation and Pollution Control, College of Environmental Sciences and Engineering, Peking University, Beijing 100871, China; orcid.org/0000-0002-6404-9263

Li Li – School of Public Health, University of Nevada Reno, Reno, Nevada 89557, United States; orcid.org/0000-0002-5157-7366

Shaoxuan Zhang – State Key Joint Laboratory for Environmental Simulation and Pollution Control, College of Environmental Sciences and Engineering, Peking University, Beijing 100871, China

Complete contact information is available at:
<https://pubs.acs.org/10.1021/acs.estlett.4c00306>

Notes

The authors declare no competing financial interest.

ACKNOWLEDGMENTS

C.C., S.Z., and J.L. are grateful for funding from the State Key Joint Laboratory for Environmental Simulation and Pollution Control of China. C.C. and F.W. are grateful for funding from the Natural Sciences and Engineering Research Council of Canada.

REFERENCES

- (1) Chen, C. K.; Chen, A. N.; Zhan, F. Q.; Wania, F.; Zhang, S. X.; Li, L.; Liu, J. G. Global Historical Production, Use, In-Use Stocks, and Emissions of Short-, Medium-, and Long-Chain Chlorinated Paraffins. *Environ. Sci. Technol.* **2022**, *56* (12), 7895–7904.
- (2) Breivik, K.; Sweetman, A.; Pacyna, J. M.; Jones, K. C. Towards a global historical emission inventory for selected PCB congeners—A mass balance approach: 3. An update. *Sci. Total Environ.* **2007**, *377* (2–3), 296–307.
- (3) Li, L.; Chen, C.; Li, D.; Breivik, K.; Abbasi, G.; Li, Y.-F. What do we know about the production and release of persistent organic pollutants in the global environment? *Environ. Sci. Adv.* **2023**, *2* (1), 55–68.
- (4) Glüge, J.; Schinkel, L.; Hungerbühler, K.; Cariou, R.; Bogdal, C. Environmental Risks of Medium-Chain Chlorinated Paraffins (MCCPs): A Review. *Environ. Sci. Technol.* **2018**, *52* (12), 6743–6760.
- (5) Jiang, L.; Gao, W.; Ma, X. D.; Wang, Y. J.; Wang, C.; Li, Y. M.; Yang, R. Q.; Fu, J. J.; Shi, J. B.; Zhang, Q. H.; Wang, Y. W.; Jiang, G. B. Long-Term Investigation of the Temporal Trends and Gas/Particle Partitioning of Short- and Medium-Chain Chlorinated Paraffins in Ambient Air of King George Island, Antarctica. *Environ. Sci. Technol.* **2021**, *55* (1), 230–239.
- (6) van Mourik, L. M.; Gaus, C.; Leonards, P. E. G.; de Boer, J. Chlorinated paraffins in the environment: A review on their production, fate, levels and trends between 2010 and 2015. *Chemosphere* **2016**, *155*, 415–428.
- (7) Gawor, A.; Wania, F. Using quantitative structural property relationships, chemical fate models, and the chemical partitioning space to investigate the potential for long range transport and bioaccumulation of complex halogenated chemical mixtures. *Environ. Sci. Process. Impacts* **2013**, *15* (9), 1671–1684.
- (8) Reth, M.; Ciric, A.; Christensen, G. N.; Heimstad, E. S.; Oehme, M. Short- and medium-chain chlorinated paraffins in biota from the European Arctic - differences in homologue group patterns. *Sci. Total Environ.* **2006**, *367* (1), 252–260.
- (9) Yuan, B.; McLachlan, M. S.; Roos, A. M.; Simon, M.; Strid, A.; de Wit, C. A. Long-Chain Chlorinated Paraffins Have Reached the Arctic. *Environ. Sci. Technol. Lett.* **2021**, *8* (9), 753–759.
- (10) Iozza, S.; Müller, C. E.; Schmid, P.; Bogdal, C.; Oehme, M. Historical profiles of chlorinated paraffins and polychlorinated biphenyls in a dated sediment core from Lake Thun (Switzerland). *Environ. Sci. Technol.* **2008**, *42* (4), 1045–1050.
- (11) Muir, D.; Bennie, D.; Teixeira, C.; Fisk, A.; Tomy, G.; Stern, G.; Whittle, M. Short chain chlorinated paraffins: Are they persistent and bioaccumulative? In *Persistent, Bioaccumulative, and Toxic Chemicals II*; ACS Symposium Series Vol. 773; American Chemical Society, 2000; pp 184–202.
- (12) Yuan, B.; Brüchert, V.; Sobek, A.; de Wit, C. A. Temporal Trends of C8-C36 Chlorinated Paraffins in Swedish Coastal Sediment Cores over the Past 80 Years. *Environ. Sci. Technol.* **2017**, *51* (24), 14199–14208.
- (13) Fisk, A. T.; Tomy, G. T.; Cymbalysty, C. D.; Muir, D. C. G. Dietary accumulation and quantitative structure-activity relationships for depuration and biotransformation of short (C10), medium (C14), and long (C18) carbon-chain polychlorinated alkanes by juvenile rainbow trout (*Oncorhynchus mykiss*). *Environ. Toxicol. Chem.* **2000**, *19* (6), 1508–1516.
- (14) Houde, M.; Muir, D. C. G.; Tomy, G. T.; Whittle, D. M.; Teixeira, C.; Moore, S. Bioaccumulation and trophic magnification of short- and medium-chain chlorinated paraffins in food webs from Lake Ontario and Lake Michigan. *Environ. Sci. Technol.* **2008**, *42* (10), 3893–3899.
- (15) Brooke, D.; Crookes, M. Case study on toxicological interactions of chlorinated paraffins. In *Seventh Meeting, Persistent Organic Pollutants Review Committee*; United Nation Environment Programme, 2011; Geneva.
- (16) Chen, S. S.; Gong, Y. F.; Luo, Y.; Cao, R.; Yang, J. J.; Cheng, L.; Gao, Y.; Zhang, H. J.; Chen, J. P.; Geng, N. B. Toxic effects and toxicological mechanisms of chlorinated paraffins: A review for insight into species sensitivity and toxicity difference. *Environ. Int.* **2023**, *178*, 108020.
- (17) Thompson, R.; Smyth, D.; Gillings, E. Medium-chain chlorinated paraffin (52% chlorinated, C14–17): Effects in sediment on the survival, growth and sexual development of the freshwater amphipod, *Hyalella azteca*. In *AstraZeneca Confidential Report BL7469/B*; UK Environment Agency, 2003.
- (18) Brooke, D.; Crookes, M.; Merckel, D. *Environmental risk assessment: long-chain chlorinated paraffins*; Environment Agency: Bristol, UK, 2009.
- (19) UNEP. *Report of the Conference of the Parties to the Stockholm Convention on Persistent Organic Pollutants on the work of its eighth meeting*; United Nation Environment Programme: Geneva, Switzerland, 2017.
- (20) UNEP. *Draft risk management evaluation: chlorinated paraffins with carbon chain lengths in the range C14–17 and chlorination levels at or exceeding 45% chlorine by weight*; United Nation Environment Programme: Rome, Italy, 2023.

- (21) Gao, Y.; Zhang, H. J.; Su, F.; Tian, Y. Z.; Chen, J. P. Environmental Occurrence and Distribution of Short Chain Chlorinated Paraffins in Sediments and Soils from the Liaohe River Basin, P. R. China. *Environ. Sci. Technol.* **2012**, *46* (7), 3771–3778.
- (22) Iino, F.; Takasuga, T.; Senthilkumar, K.; Nakamura, N.; Nakanishi, J. Risk assessment of short-chain chlorinated paraffins in Japan based on the first market basket study and species sensitivity distributions. *Environ. Sci. Technol.* **2005**, *39* (3), 859–866.
- (23) Zhou, Y. H.; Asplund, L.; Yin, G.; Athanassiadis, I.; Wideqvist, U.; Bignert, A.; Qiu, Y. L.; Zhu, Z. L.; Zhao, J. F.; Bergman, A. Extensive organohalogen contamination in wildlife from a site in the Yangtze River Delta. *Sci. Total Environ.* **2016**, *554*, 320–328.
- (24) Li, Q. L.; Li, J.; Wang, Y.; Xu, Y.; Pan, X. H.; Zhang, G.; Luo, C. L.; Kobara, Y.; Nam, J. J.; Jones, K. C. Atmospheric Short-Chain Chlorinated Paraffins in China, Japan, and South Korea. *Environ. Sci. Technol.* **2012**, *46* (21), 11948–11954.
- (25) Li, T.; Gao, S. X.; Ben, Y. J.; Zhang, H.; Kang, Q. Y.; Wan, Y. Screening of Chlorinated Paraffins and Unsaturated Analogues in Commercial Mixtures: Confirmation of Their Occurrences in the Atmosphere. *Environ. Sci. Technol.* **2018**, *52* (4), 1862–1870.
- (26) Wu, J.; Gao, W.; Liang, Y.; Fu, J. J.; Gao, Y.; Wang, Y. W.; Jiang, G. B. Spatiotemporal Distribution and Alpine Behavior of Short Chain Chlorinated Paraffins in Air at Shergyla Mountain and Lhasa on the Tibetan Plateau of China. *Environ. Sci. Technol.* **2017**, *51* (19), 11136–11144.
- (27) Wu, J.; Gao, W.; Liang, Y.; Fu, J. J.; Shi, J. B.; Lu, Y.; Wang, Y. W.; Jiang, G. B. Short- and medium-chain chlorinated paraffins in multi-environmental matrices in the Tibetan Plateau environment of China: A regional scale study. *Environ. Int.* **2020**, *140*, 105767.
- (28) EC. *Technical Guidance Document on Risk Assessment - Part II*; European Commission, Joint Research Center, Institute for Health and Consumer Protection, European Chemicals Bureau: Ispra, Italy, 2003.
- (29) Wettstad, J. The Convention on Long-Range Transboundary Air Pollution (CLRTAP). In *Environmental Regime Effectiveness*; MIT Press, 2001; Vol. 42, pp 197–221.
- (30) Wöhrschimmel, H.; MacLeod, M.; Hungerbühler, K. Global multimedia source-receptor relationships for persistent organic pollutants during use and after phase-out. *Atmos. Pollut. Res.* **2012**, *3* (4), 392–398.
- (31) Corbitt, E. S.; Jacob, D. J.; Holmes, C. D.; Streets, D. G.; Sunderland, E. M. Global Source-Receptor Relationships for Mercury Deposition Under Present-Day and 2050 Emissions Scenarios. *Environ. Sci. Technol.* **2011**, *45* (24), 10477–10484.
- (32) MacLeod, M.; von Waldow, H.; Tay, P.; Armitage, J. M.; Wöhrschimmel, H.; Riley, W. J.; McKone, T. E.; Hungerbühler, K. BETR global - A geographically-explicit global-scale multimedia contaminant fate model. *Environ. Pollut.* **2011**, *159* (5), 1442–1445.
- (33) MacLeod, M.; Riley, W. J.; McKone, T. E. Assessing the influence of climate variability on atmospheric concentrations of polychlorinated biphenyls using a global-scale mass balance model (BETR-Global). *Environ. Sci. Technol.* **2005**, *39* (17), 6749–6756.
- (34) Chen, C. K.; Li, L.; Liu, J. Z.; Liu, J. G. Global environmental fate of short-chain chlorinated paraffins: Modeling with a single vs. multiple sets of physicochemical properties. *Sci. Total Environ.* **2019**, *666*, 423–430.
- (35) Armitage, J. M.; MacLeod, M.; Cousins, I. T. Modeling the Global Fate and Transport of Perfluorooctanoic acid (PFOA) and Perfluorooctanoate (PFO) Emitted from Direct Sources Using a Multispecies Mass Balance Model. *Environ. Sci. Technol.* **2009**, *43* (4), 1134–1140.
- (36) Genualdi, S.; Harner, T.; Cheng, Y.; MacLeod, M.; Hansen, K. M.; van Egmond, R.; Shoeib, M.; Lee, S. C. Global Distribution of Linear and Cyclic Volatile Methyl Siloxanes in Air. *Environ. Sci. Technol.* **2011**, *45* (8), 3349–3354.
- (37) Breivik, K.; Armitage, J. M.; Wania, F.; Sweetman, A. J.; Jones, K. C. Tracking the Global Distribution of Persistent Organic Pollutants Accounting for E-Waste Exports to Developing Regions. *Environ. Sci. Technol.* **2016**, *50* (2), 798–805.
- (38) Li, L.; Wania, F. Elucidating the Variability in the Hexabromocyclododecane Diastereomer Profile in the Global Environment. *Environ. Sci. Technol.* **2018**, *52* (18), 10532–10542.
- (39) Li, L.; Wania, F. Tracking chemicals in products around the world: introduction of a dynamic substance flow analysis model and application to PCBs. *Environ. Int.* **2016**, *94*, 674–686.
- (40) Li, L.; Liu, J. G.; Hu, J. X. Global Inventory, Long-Range Transport and Environmental Distribution of Dicofol. *Environ. Sci. Technol.* **2015**, *49* (1), 212–222.
- (41) Krogseth, I. S.; Breivik, K.; Arnot, J. A.; Wania, F.; Borgen, A. R.; Schlabach, M. Evaluating the environmental fate of short-chain chlorinated paraffins (SCCPs) in the Nordic environment using a dynamic multimedia model. *Environ. Sci. Process. Impacts* **2013**, *15* (12), 2240–2251.
- (42) Endo, S. Refinement and extension of COSMO-RS-trained fragment contribution models for predicting the partition properties of C10–20 chlorinated paraffin congeners. *Environ. Sci. Process. Impacts* **2021**, *23* (6), 831–843.
- (43) Endo, S.; Hammer, J. Predicting Partition Coefficients of Short-Chain Chlorinated Paraffin Congeners by COSMO-RS-Trained Fragment Contribution Models. *Environ. Sci. Technol.* **2020**, *54* (23), 15162–15169.
- (44) Jensen, S. R.; Brown, W. A.; Heath, E.; Cooper, D. G. Characterization of polychlorinated alkane mixtures - a Monte Carlo modeling approach. *Biodegradation* **2007**, *18* (6), 703–717.
- (45) Chen, C.; Li, L.; Endo, S.; Jiang, S.; Wania, F. Are We Justified in Modeling Human Exposure to Chlorinated Paraffin Mixtures Using the Average Properties of Congeners and Homologues? *Environ. Sci. Technol.* **2024**, *58* (10), 4535–4544.
- (46) U.S. EPA. *Estimation Programs Interface suite for Microsoft Windows, v4.11*; United States Environmental Protection Agency: Washington, DC, USA, 2012.
- (47) Arnot, J.; Gouin, T.; Mackay, D. *Practical methods for estimating environmental biodegradation rates*; Canadian Environmental Modelling Centre: Peterborough, Ontario, 2005.
- (48) Bogdal, C.; Niggeler, N.; Glüge, J.; Diefenbacher, P. S.; Wächter, D.; Hungerbühler, K. Temporal trends of chlorinated paraffins and polychlorinated biphenyls in Swiss soils. *Environ. Pollut.* **2017**, *220*, 891–899.
- (49) Zhang, C. X.; Chang, H.; Wang, H. P.; Zhu, Y. R.; Zhao, X. L.; He, Y.; Sun, F. H.; Wu, F. C. Spatial and Temporal Distributions of Short-, Medium-, and Long-Chain Chlorinated Paraffins in Sediment Cores from Nine Lakes in China. *Environ. Sci. Technol.* **2019**, *53* (16), 9462–9471.
- (50) Marvin, C. H.; Painter, S.; Tomy, G. T.; Stern, G. A.; Braekevelt, E.; Muir, D. C. G. Spatial and temporal trends in short-chain chlorinated paraffins in Lake Ontario sediments. *Environ. Sci. Technol.* **2003**, *37* (20), 4561–4568.
- (51) Bohlin-Nizzetto, P.; Aas, W.; Halvorsen, H. L.; Nikiforov, V.; Pfaffhuber, K. A. *Monitoring of environmental contaminants in air and precipitation. Annual report 2020*. (NILU report 12/2021; Norwegian Environment Agency M-2060/2021). Kjeller: NILU, 2021.
- (52) Huang, P.; Gong, S. L.; Zhao, T. L.; Neary, L.; Barrie, L. A. GEM/POPs: a global 3-D dynamic model for semi-volatile persistent organic pollutants - Part 2: Global transports and budgets of PCBs. *Atmos. Chem. Phys.* **2007**, *7* (15), 4015–4025.
- (53) Chen, C. K.; Chen, A. N.; Li, L.; Peng, W. Y.; Weber, R.; Liu, J. G. Distribution and Emission Estimation of Short- and Medium-Chain Chlorinated Paraffins in Chinese Products through Detection-Based Mass Balancing. *Environ. Sci. Technol.* **2021**, *55* (11), 7335–7343.
- (54) Breivik, K.; Eckhardt, S.; McLachlan, M. S.; Wania, F. Introducing a nested multimedia fate and transport model for organic contaminants (NEM). *Environ. Sci. Process. Impacts* **2021**, *23* (8), 1146–1157.
- (55) Li, Y. F.; Ma, W. L.; Yang, M. Prediction of gas/particle partitioning of polybrominated diphenyl ethers (PBDEs) in global air: A theoretical study. *Atmos. Chem. Phys.* **2015**, *15* (4), 1669–1681.

- (56) Zhao, F. Y.; Riipinen, I.; MacLeod, M. Steady-State Mass Balance Model for Predicting Particle-Gas Concentration Ratios of PBDEs. *Environ. Sci. Technol.* **2021**, *55* (14), 9425–9433.
- (57) Göktaş, R. K.; MacLeod, M. Remoteness from sources of persistent organic pollutants in the multi-media global environment. *Environ. Pollut.* **2016**, *217*, 33–41.
- (58) Liu, Q. F.; Liggio, J.; Wu, D. M.; Saini, A.; Halappanavar, S.; Wentzell, J. J. B.; Harner, T.; Li, K.; Lee, P.; Li, S. M. Experimental Study of OH-Initiated Heterogeneous Oxidation of Organophosphate Flame Retardants: Kinetics, Mechanism, and Toxicity. *Environ. Sci. Technol.* **2019**, *53* (24), 14398–14408.
- (59) Liu, Q. F.; Liggio, J.; Wentzell, J.; Lee, P.; Li, K.; Li, S. M. Atmospheric OH Oxidation Chemistry of Particulate Liquid Crystal Monomers: An Emerging Persistent Organic Pollutant in Air. *Environ. Sci. Technol. Lett.* **2020**, *7* (9), 646–652.
- (60) Stocker, J.; Scheringer, M.; Wegmann, F.; Hungerbühler, K. Modeling the effect of snow and ice on the global environmental fate and long-range transport potential of semivolatile organic compounds. *Environ. Sci. Technol.* **2007**, *41* (17), 6192–6198.